Ternary Lead Chalcogenide Alloys for Mid-Infrared Detectors

Citation: Su, P. et al. "Ternary Lead Chalcogenide Alloys for Mid-Infrared Detectors." Journal of Electronic Materials 49, 8 (April 2020): 4577–4580 © 2020 The Minerals, Metals & Materials Society

As Published: https://doi.org/10.1007/s11664-020-08114-w

Publisher: Springer Science and Business Media LLC

Persistent URL: https://hdl.handle.net/1721.1/130396

Version: Author's final manuscript: final author's manuscript post peer review, without publisher's formatting or copy editing

Ternary Lead Chalcogenide Alloys for Mid-Infrared Detectors

Cite this article as: P. Su, R. Pujari, V. Boodhoo, S. Aggarwal, P. Bhattacharya, O. Maksimov, K. Wada, S. Merlo, H. B. Bhandari, L. C. Kimerling and A. Agarwal, Ternary Lead Chalcogenide Alloys for Mid-Infrared Detectors, Journal of Electronic Materials https://doi.org/10.1007/s11664-020-08114-w

Ternary Lead Chalcogenide Alloys for Mid-Infrared Detectors

P. Su[1,a)], R. Pujari[1)], V. Boodhoo[1)], S. Aggarwal[1)], P. Bhattacharya[2)], O. Maksimov[2)], K. Wada[1)], S. Merlo[3)], H. B. Bhandari[2)], L. C. Kimerling[1)], and A. Agarwal[1,4)]

[1]*Department of Materials Science and Engineering, Massachusetts Institute of Technology, Cambridge, Massachusetts 02139, USA*

[2]*Radiation Monitoring Devices, Inc., Watertown, Massachusetts 02472, USA*

[3]*Department of Electrical, Computer, and Biomedical Engineering, University of Pavia, 27100 Pavia, Italy*

[4]*Materials Research Laboratory, Massachusetts Institute of Technology, Cambridge, Massachusetts 02139, USA*

ABSTRACT

We demonstrate thin films of $PbSe_{1-x}S_x$ and $PbSe_{1-x}Te_x$ lead chalcogenide ternary alloys as infrared detectors. The films were deposited on single crystal BaF_2 substrates using physical vapor deposition (PVD). The detector detectivity in the wavelength range from 1 μm to 5 μm was measured at -40°C, and all films showed a photoresponse signal more than an order of magnitude larger than their noise. The detectivity spectra were used to assess the tunability of the band gap from mixing the lead chalcogenide binaries. The $PbSe_{1-x}S_x$ system showed tunability that followed Vegard's law, while the $PbSe_{1-x}Te_x$ system showed tunability with a bowing parameter of -0.096 eV. Comparisons to measurements from the literature taken at room temperature suggest that the bowing parameter decreases with decreasing temperature and the band gap temperature coefficient with respect to composition also shows bowing.

Keywords: lead chalcogenide ternary alloys, infrared detectors, physical vapor deposition, tunable band gap.

[a)] Author to whom correspondence should be addressed. Electronic mail: peterxsu@mit.edu.

INTRODUCTION

The binary lead chalcogenides (PbS, PbSe, PbTe) are among the first discovered practical infrared detector materials [1]. They are also generally miscible with each other, with the $PbSe_{1-x}S_x$ system being completely miscible at equilibrium at all temperatures and the $PbSe_{1-x}Te_x$ system only showing a miscibility gap in equilibrium starting at around 300°C [2,3]. Since all three binary lead chalcogenides are direct band gap semiconductors with the same crystal structure [4], the ternary alloys formed by mixing any two of the binaries promise a way to tune the band gap across the mid-infrared spectrum. This would potentially create detectors with reduced noise, and therefore higher detectivity (D*), compared to PbSe, the smallest bandgap lead chalcogenide, due to reduced thermal generation of carriers caused by the larger band gap, while still allowing the detector to work at the wavelengths needed for a particular application.

Previous work on the $PbSe_{1-x}S_x$ and $PbSe_{1-x}Te_x$ systems have deposited the materials in thin film form using solution growth [5,6], spray deposition [7], physical vapor deposition [8–11], and molecular beam and liquid phase epitaxy [12,13]. Physical vapor deposition (PVD) is the only technique by which these materials have been deposited where any substrate can be used (unlike epitaxial techniques) and that is compatible with the full range of standard lithographic techniques such as liftoff (unlike solution-based techniques), enabling PVD deposited films to be patterned at very small length scales for numerous applications, including integrated photonic circuits operating in the infrared wavelength region.

EXPERIMENTAL PROCEDURES

In this work, we deposited $PbSe_{1-x}S_x$ and $PbSe_{1-x}Te_x$ ternary alloys using PVD on single crystal (111) BaF_2 substrates. The deposition was performed at a base pressure of 2.7×10^{-8} kPa.

All thin films were evaporated from single sources created by alloying the bulk binary compounds. The source temperature was 420°C - 450°C, resulting in a pressure during deposition of about 6.7 x 10^{-7} kPa, substrate temperature of about 200°C induced by thermal radiation from the source, and a deposition rate of about 10 nm/min. Film composition was measured using Wavelength-Dispersive X-Ray Spectroscopy (WDS). Majority carrier type, concentration, and mobility were measured at room temperature using the van der Pauw technique [14].

To test the photodetection capabilities of the deposited thin films and measure their band gaps, 300 nm of tin, which was previously used by Wang et al. [15], was deposited on the thin films via a shadow mask in the pattern shown in Figure 1a and 1b. The area of the detectors is 1 mm x 2 mm between the tin contacts. I-V measurements were taken on all samples to confirm the ohmic nature of the contacts, and an example result is shown in Figure 1c.

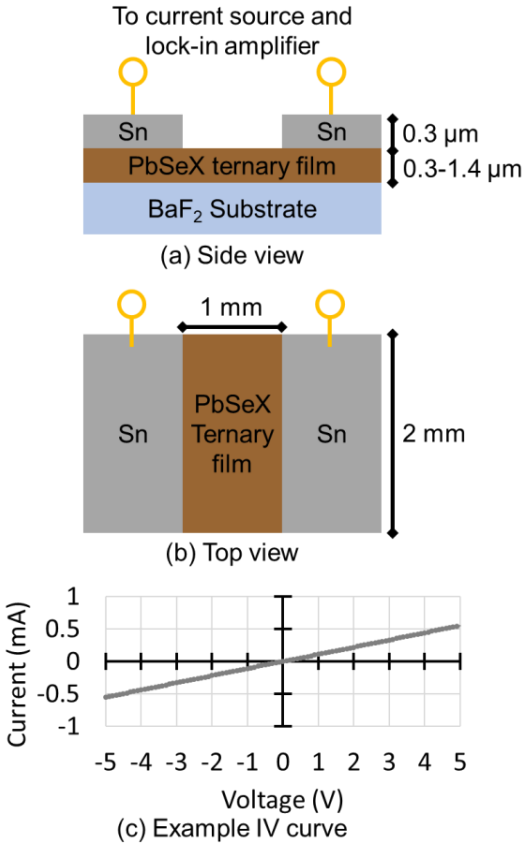

Fig. 1. (a) Side view and (b) top view schematics of the structure of the photoconductors made from the lead chalcogenide thin films. The detector contacts are made of tin, and the detector area is 1 mm by 2 mm. (c) Example I-V curve showing ohmic behavior of tin contacts.

The photoconductor samples were mounted on a thermoelectric cooler placed inside a vacuum chamber to allow the samples to be cooled to -40°C during testing without condensation. The vacuum chamber included a CaF_2 window to let infrared light reach the sample. Broadband light from a 140 W glowbar was modulated at 100 Hz with a chopper and coupled into a grating monochromator (Model 77700 MS257 1/4 m Monochromator, Newport). An aluminum mirror then focused the light leaving the monochromator onto either the sample or a broadband pyroelectric reference detector with a known response, which measured the optical power incident on the sample. All samples were biased using a constant current from a Keithley 6220

current source, and the photovoltage due to the chopped light was amplified by a lock-in amplifier with an effective noise bandwidth of 0.2 Hz.

RESULTS AND DISCUSSIONS

Film Characterization

Table I shows the compositions of the deposited thin films measured using Wavelength Dispersive X-ray Spectroscopy (WDS). The films are named after their compositions, with PSS# being a $PbSe_{1-x}S_x$ alloy with # at% PbS and PST# being a $PbSe_{1-x}Te_x$ alloy with # at% PbTe. Both ternary alloys show significant compositional tunability.

Table I. Compositions, electrical, and optical properties of the $PbSe_{1-x}S_x$ and $PbSe_{1-x}Te_x$ ternary alloys films deposited using PVD on uncooled BaF_2 substrates. The D* is the Johnson-noise-limited D*.

Sample Name	Film Composition (measured via WDS)	Carrier Type	Carrier Concentration (cm^{-3})	Carrier Mobility ($cm^2/V/s$)	Peak D* @ -40°C & 1 mA ($cm\sqrt{Hz}/W$)	Band Gap @ -40°C (eV)
PSS23	$PbSe_{0.77}S_{0.23}$	N	2.36×10^{19}	0.22	1.43×10^{7}	0.266
PSS42	$PbSe_{0.58}S_{0.42}$	N	3.06×10^{18}	4.03	7.34×10^{7}	0.297
PST12	$PbSe_{0.88}Te_{0.12}$	P	8.56×10^{18}	1.82	1.34×10^{8}	0.267
PST39	$PbSe_{0.61}Te_{0.39}$	P	8.29×10^{16}	58.6	7.09×10^{8}	0.278

The detectivity spectra of the samples, assuming Johnson-noise-limited behavior, are shown in Figure 2, normalized to 1 to more clearly show the differences in band gap of the samples. All films showed a photovoltage signal at least an order of magnitude above their noise level.

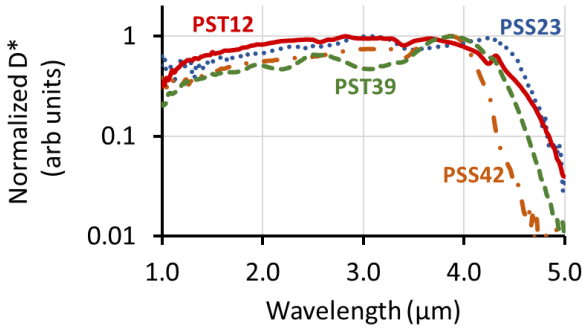

Fig. 2. Johnson-noise-limited detectivity as a function of wavelength of the $PbSe_{1-x}S_x$ and $PbSe_{1-x}Te_x$ thin films taken at -40°C, normalized to 1. All samples showed a photoresponse more than an order of magnitude above noise levels.

The samples also showed significant differences in peak Johnson-noise-limited detectivities at 1 mA of bias current, as shown in Table I. To get a better insight into the causes of these differences, the majority carrier types, concentrations, and mobilities were measured and the results are shown in Table I. As expected for a photoconductor under constant current bias, the detectivity generally increases as the carrier concentration decreases [16]. Additional studies are ongoing to determine why these films showed such different carrier concentrations and detectivities.

Bandgap Determination

The spectral detectivities of the films were used to determine the band gaps of the films, using the relationship:

$$\alpha \propto \ D^* \cdot E_{ph}\big|_{\text{near } E_g} \#(1)$$

where α is the absorption coefficient, D^* is the detectivity of the film, E_{ph} is the energy of the photon at a given wavelength, and E_g is the band gap energy. This can be derived from the following two relationships:

$$\alpha \propto -\ln\left(1-\frac{photons_{absorbed}}{photons_{incident}}\right) \approx \left.\frac{photons_{absorbed}}{photons_{incident}}\right|_{near\ E_g} \#(2)$$

$$D^* \propto \frac{photoelectrons}{photons_{incident}\cdot E_{ph}} = \frac{photons_{absorbed}}{photons_{incident}}\cdot\frac{\eta}{E_{ph}} \#(3)$$

where η is the quantum efficiency, $photons_{incident}$ is the number of impinging photons on the film, $photons_{absorbed}$ is the number of absorbed photons, and *photoelectrons* is the number of photogenerated electrons. Equation 2 shows that the absorption coefficient near the band gap is proportional to the fraction of photons absorbed, and Equation 3 shows that the fraction of photons absorbed is directly proportional to the detectivity of the film multiplied by the photon energy, assuming a constant quantum efficiency versus photon energy. All the lead chalcogenides are direct band gap materials, so the absorption coefficient squared is directly proportional to the photon energy minus the band gap at photon energies slightly above the band gap. Therefore, plotting the square of the detectivity multiplied by the photon energy as a function of the photon energy, we can use a linear fitting to extrapolate the band gap, as shown in the example in Figure 3a. The band gaps measured in this manner are listed in Table I and plotted in Figures 3b and 3c. The band gaps of the binary end members (PbS, PbSe, and PbTe) at -40°C were calculated from room temperature band gaps and band gap temperature coefficients found in Madelung [4].

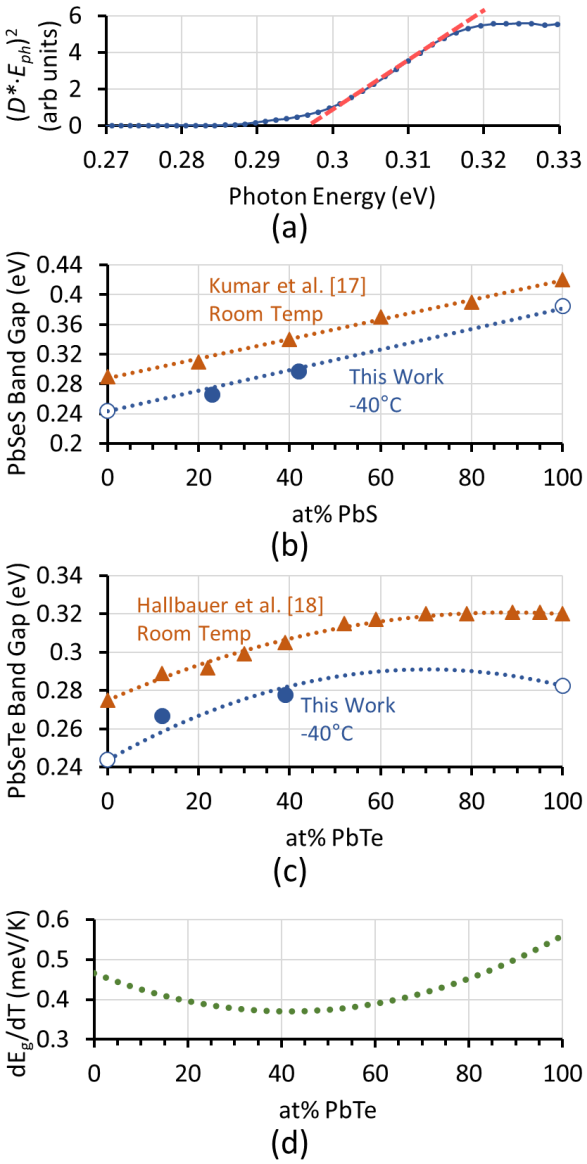

Fig. 3. (a) Result of a band gap measurement, taken on sample PSS42, showing the linear relationship between the absorption squared and photon energy near the band gap. The extrapolated band gap value is 0.297 eV. (b) and (c) Band gaps measured at -40°C plotted against composition for both the (b) $PbSe_{1-x}S_x$ and (c) $PbSe_{1-x}Te_x$ materials systems deposited in this work, compared to previous measurements done on thin films by Kumar et al. [17] and Hallbauer et al. [18] at room temperature. The band gaps of the binary end members (PbS, PbSe, and PbTe) at -40°C were calculated from values found in Madelung [4]. The $PbSe_{1-x}Te_x$ system shows a best fit bowing parameter of -0.096 eV at -40°C. (d) Band gap temperature coefficient versus composition from comparing Hallbauer et al. and our work.

The $PbSe_{1-x}S_x$ system shows a linear relationship between composition and band gap, which closely matches expectations from Vegard's law and the trend found from Fourier Transform

Infra-Red (FTIR) measurements at room temperature by Kumar et al. [17] on $PbSe_{1-x}S_x$ thin films. The $PbSe_{1-x}Te_x$ system, however, shows very strong bowing, with a best fit bowing parameter of -0.096 eV. This behavior matches the trend found from FTIR measurements at room temperature by Hallbauer et al. [18] on $PbSe_{1-x}Te_x$ thin films and by Yamini et al. [19] on $PbSe_{1-x}Te_x$ powders, but the bowing parameter we find at -40°C is larger in magnitude than the ones at room temperature measured by Hallbauer et al. (~ -0.059 eV) and Yamini et al. (~ -0.053 eV), suggesting that the bowing parameter decreases as the temperature decreases. This hypothesis is further confirmed by data from Preier [20] at 77 K (-196°C), which show a bowing parameter of ~ -0.147 eV (using the fact that lattice parameter for $PbSe_{1-x}Te_x$ varies linearly with composition [18,19]). All three sets of measurements show that the low atomic fraction PbTe compositions, where most of the band gap tunability occurs, are significantly more important for tunable detectors using the $PbSe_{1-x}Te_x$ system. Comparison between our experimental results at -40°C and other experimental results taken at room temperature also clearly shows a positive band gap temperature coefficient, similar to the binary lead chalcogenides [4]. Figure 3d shows the band gap temperature coefficient versus composition calculated by comparing the measurements from Hallbauer et al. and our work. The band gap temperature coefficient also shows significant bowing, which is implied by the changing bowing parameter of the band gap with temperature.

CONCLUSIONS

In conclusion, we have demonstrated viable infrared detectors made with different alloys of the $PbSe_{1-x}S_x$ and $PbSe_{1-x}Te_x$ material systems deposited using PVD. The thin films showed a photoresponse signal at -40°C more than an order of magnitude higher than their noise level. The detectivity generally increases as the carrier concentration decreases. The band gaps can also be

tuned by changing the composition, with the $PbSe_{1-x}S_x$ system showing a behavior matching Vegard's law and the $PbSe_{1-x}Te_x$ system having a bowing parameter of -0.096 eV at -40°C. Comparison to measurement results from the literature taken at room temperature suggest that the bowing parameter decreases with decreasing temperature, resulting in bowing in the band gap temperature coefficient with respect to composition. The successful fabrication of working photodetectors with tunable band gaps indicates that ternary lead chalcogenide alloys deposited via PVD are promising materials for tunable infrared detector applications.

ACKNOWLEDGEMENTS

Funding from ONR SBIR award number N68335-19-C-0070 is gratefully acknowledged. This work made use of the MRSEC Shared Experimental Facilities at MIT, supported by the National Science Foundation under Award No.DMR-1419807.

CONFLICT OF INTEREST

The authors declare that they have no conflict of interest.

REFERENCES

1. A. Rogalski, Opto-Electronics Rev. **20**, 279 (2012).

2. H. Liu and L. L. Y. Chang, Mineral. Mag. **58**, 567 (1994).

3. R. J. Korkosz, T. C. Chasapis, S. Lo, J. W. Doak, Y. J. Kim, C.-I. Wu, E. Hatzikraniotis, T. P. Hogan, D. N. Seidman, C. Wolverton, V. P. Dravid, and M. G. Kanatzidis, J. Am. Chem. Soc. **136**, 3225 (2014).

4. O. Madelung, in *Semicond. Data Handb.* (2004), pp. 566–605.

5. Y. S. Sarma, H. N. Acharya, and N. K. Misra, Thin Solid Films **90**, L43 (1982).

6. Y. S. Sarma, H. N. Acharya, and N. K. Misra, Infrared Phys. **24**, 425 (1984).

7. H. Abouelkhair, P. N. Figueiredo, S. R. Calhoun, C. J. Fredricksen, I. O. Oladeji, E. M. Smith, J. W. Cleary, and R. E. Peale, MRS Adv. **3**, 291 (2018).

8. B. A. Riggs, J. Electrochem. Soc. **114**, 708 (1967).

9. S. Kumar, B. Lal, P. Aghamkar, and M. Husain, J. Alloys Compd. **488**, 334 (2009).

10. S. Kumar, B. Lal, S. Rohilla, P. Aghamkar, and M. Husain, J. Alloys Compd. **505**, 135 (2010).

11. A. Hmood, A. Kadhim, and H. Abu Hassan, Superlattices Microstruct. **51**, 825 (2012).

12. V. F. Chishko, V. T. Hryapov, I. L. Kasatkin, V. V. Osipov, and O. V. Smolin, Infrared Phys. **33**, 275 (1992).

13. E. Kapon, A. Zussman, and A. Katzir, Appl. Phys. Lett. **44**, 275 (1984).

14. L. J. van der Pauw, Philips Res. Rep. **13**, 1 (1958).

15. J. Wang, J. Hu, P. Becla, A. M. Agarwal, and L. C. Kimerling, J. Appl. Phys. **110**, 083719 (2011).

16. J. Wang, Resonant-Cavity-Enhanced Multispectral Infrared Photodetectors for Monolithic Integration on Silicon, 2010.

17. S. Kumar, M. A. Majeed Khan, S. A. Khan, and M. Husain, Opt. Mater. (Amst). **25**, 25 (2004).

18. A. Hallbauer, T. Schwarzl, R. T. Lechner, and G. Springholz, Proc. GMe Forum 2003 109 (2003).

19. S. A. Yamini, V. Patterson, and R. Santos, ACS Omega **2**, 3417 (2017).

20. H. Preier, Semicond. Sci. Technol. **5**, S12 (1990).